IEEE Access
Multidisciplinary | Rapid Review | Open Access Journal

Received April 6, 2018, accepted May 5, 2018, date of publication May 21, 2018, date of current version June 29, 2018.

Digital Object Identifier 10.1109/ACCESS.2018.2838544

Implementation of a Ball and Plate Control System Using Sliding Mode Control

HEESEUNG BANG AND YOUNG SAM LEE
Department of Electrical Engineering, Inha University, Incheon 22212, South Korea
Corresponding author: Young Sam Lee (lys@inha.ac.kr)

This work was supported by the Inha University Research Grant.

ABSTRACT In this paper, we propose a cost-effective implementation method of a ball and plate system as an educational kit and present the application of sliding mode control to achieve better control performance. We choose a Stewart platform with rotary actuators to manipulate the plate. We explain the construction method of the platform in detail. We use a touch panel as a sensor to obtain the positional data at a high sample rate and to make the system compact. As a main control unit, we use a Nucleo-32 board, which is a small and powerful open source hardware with a built-in floating point unit. For controller synthesis, we show a mathematical model of the ball and plate system and explain the kinematics analysis of the Stewart platform. We design a sliding mode controller that includes error integration, which makes the system robust against external disturbances. We describe the results of the simulations and the experiments and then illustrate the advantage of the applied sliding mode control compared to LQ control. The proposed system is cost-effective, can be easily built, has good control performance, and occupies a small space. For these reasons, we expect that the system can be efficiently used as an educational tool.

INDEX TERMS Ball and plate system, Stewart platform, sliding mode control (SMC).

I. INTRODUCTION

In the field of control education, motivating students and improving their comprehension have always been important topics for educators. The most effective way to enhance students' understanding is to give them the opportunity to learn through the experiments so that they can understand the control scheme through hands-on experiences. For these reasons, there are many approaches to developing educational kits and platforms for control engineering curriculums [1]–[3]. In general, unstable systems, such as ball and plate systems or inverted pendulum systems, are effective in helping students understand the effect of closed-loop control because things that are impossible without control can be made possible through control. Therefore, such systems are often more interesting and likely to increase students' motivation to learn. But unfortunately, the inverted pendulum system is not easily used for mass education. A pendulum system with a cart has a limit in rail length [4], [5], which can be damaged if the controller is not well-designed. In addition, a long rail needs a lot of space for experiments. A rotary inverted pendulum can overcome these difficulties, but the rotating pendulum can be dangerous when the system is not properly controlled. On the other hand, ball and plate systems need only a small space compared to the pendulum system, and an uncontrolled system does not produce critical damage but only drops the ball to the ground.

The ball and plate system, which is an expanded version of the ball and beam system, is also useful for verifying the controllers since researchers can apply various theories such as LQ control [6], sliding mode control (SMC) [7], hierarchical fuzzy control [8], and PID neural-network [9]. The general control purpose is to stabilize the position of the ball and to track trajectories. Most of the existing ball and plate systems use 2-DOF hardware that only can rotate with respect to the x- and y-axes and uses a vision camera to find the position of the ball. They have some disadvantages as follows: 1) They need extra computers or other micro control unit (MCU) for vision processing. 2) Most of low-cost vision cameras can capture less than 60 frames per second and so cannot be run at fast sample rates. 3) Vision processing is very weak to changes of the testing environment.

Sliding mode control (SMC) is a representative robust nonlinear control scheme that is also used in a ball and plate system. It is simple and widely used [7], [10], [11] but has

well-known chattering problems that cause mechanical and electronic damage to the systems. Researchers have found several methods for reducing chattering such as using a saturation function, fuzzy logic [12], and designing an adaptive SMC [13], [14].

In this paper, we propose an implementation method of the ball and plate control system as an education kit. Compared to the existing ball and plate system, we use a touch panel for sensing the position of the ball, and the sensing process occurs every millisecond, allowing the sensor to provide the feedback at high frequency. Furthermore, it is small and does not need any other equipment. Accordingly, the system has better portability that enables the experiments to be done in any place. The existing ball and plate control systems using SMC need to be placed exactly horizontal to the ground. On the other hand, we designed a SMC that includes an integration term to make the system robust against input disturbances. To reduce chattering, the sigmoid function is selected.

The Stewart platform is one type of 6-DOF parallel manipulator. Compared to existing ball and plate systems, the proposed system can handle more challenging motions and control problems. The Stewart platform can be made using rotary actuators or prismatic actuators. We use 6 servo motors as rotary actuators to construct the platform with low-cost.

Control education should be both theoretical and experiential [15]. The proposed method can satisfy the needs of both educators and students, such that 1) the system can be made in the lab cost-effectively, 2) students can apply various control theories without worrying about construction of the system, and 3) the experiments can be conducted anywhere, as the system occupies only a small space. For these reasons, the proposed method can effectively help educators and students who suffer from lack of good experimental systems.

The remainder of this paper is organized as follows. In Section II, the design and implementation methods are given. The mathematical model of the ball and plate system and kinematic analysis of the Stewart platform are described in Section III. Design of the SMC and the simulation are provided in Section IV. Experimental results and a comparison with LQ control are given in Section V. Finally, conclusions are drawn in Section VI.

II. DESIGN AND IMPLEMENTATION METHOD

A. MICRO-CONTROLLER UNIT

As a main MCU, we use a Nucleo-32 board, which is effective for producing low-cost prototypes. This board is small and powerful open-source hardware that is equipped with free IDE(System Workbench for STM32) and GUI-based configuration tool(STM32CubeMX). It can run at the maximum clock speed of 72MHz and has a built-in floating point unit (FPU) that is efficient for calculating the angles of 6 servo motors at every sampling time. The Nucleo-32 board can generate more than 6 PWM channels so that all servo motors can be controlled. The board is assembled on the top side of the base of the Stewart platform.

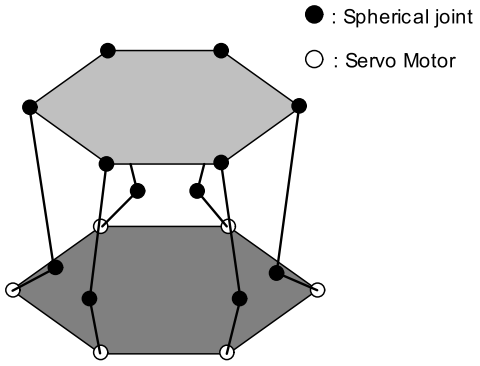

FIGURE 1. Concept of the Stewart platform with rotary actuators.

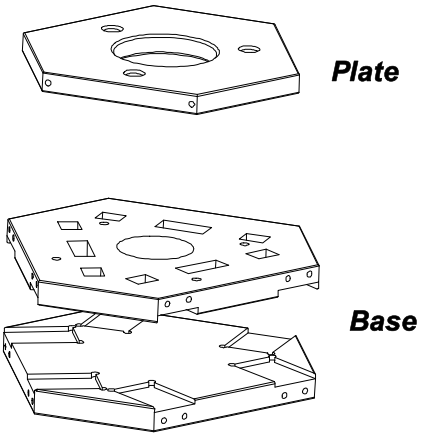

FIGURE 2. Design of the 3 parts of a Stewart platform.

B. ACTUATION PART

We use a Stewart platform as an actuation part of the system. The Stewart platform can be made using rotary actuators or prismatic actuators. In this paper, we explain an implementation method that uses rotary actuators because it is easier to apply and more cost-effective. Fig. 1 shows the conceptual diagram of the Stewart platform with rotary actuators.

We design 3 parts as shown in Fig. 2, a single part for the plate, and 2 layers for the base. We use 6 servo motors and 12 spherical joints. The servo motors used in this paper can rotate 60 degrees per 0.08 seconds at 6V. The base and plate of a Stewart platform are made of aluminum using CNC. As shown in Fig. 3, both layers of the base have 3-mm-deep rectangular slots for servo motors to be assembled easily. The system is designed small so that the experiments can be done on a desk. All the legs are made of aluminum using a metal lathe in the lab, and the length of the legs, from the center of one joint to another, is 135mm. We use horns with a length of 20mm. Fig. 4 is a picture of a lab-built ball and plate system with a Stewart platform as an actuation part.

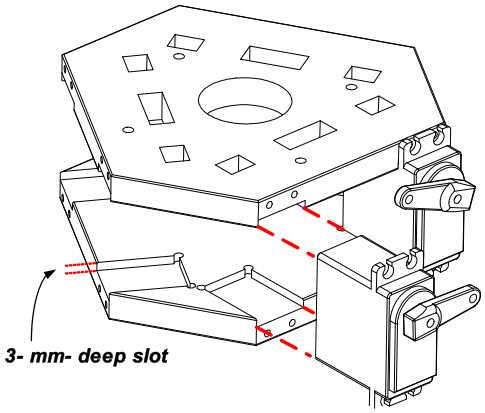

FIGURE 3. Conceptual diagram of the assembly.

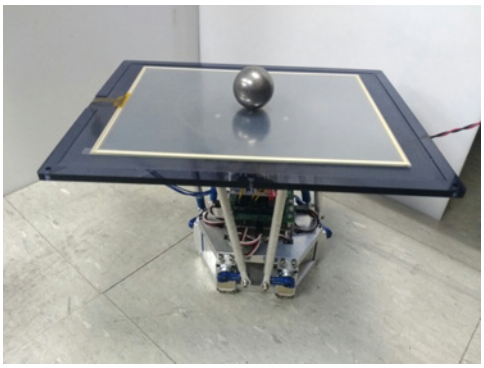

FIGURE 4. Picture of a ball and plate system with a Stewart platform as an actuation part.

C. SENSING PART

Most existing ball and plate systems use a vision camera as a sensor. But, most low-cost vision cameras capture less than 60 frames per second, and the data is highly influenced by the environment. Also, the vision process usually needs extra computers. In contrast, we use a touch panel that can obtain the position data at every millisecond and does not need any other equipment. The sensing ability varies in accordance with the size of the touch panel and weight of the ball. In this paper, we use a 10.2 inch panel and a metal ball whose diameter is 35mm and weight is about 175g.

In order to obtain the data easily, we use ADS7846E, a touch panel controller. This controller reads analog voltage, which has the information on x- and y- coordinates from the touch panel, changes the data to digital, and then sends it to the MCU through SPI communication. The controller changes the connection of the ground and VCC pin to read x- and y- values, as in (a) of Fig. 5. As shown in (b) and (c) of Fig. 5, we also read the z- value in order to determine whether or not the panel is touched. If the panel is pressed, the z- value varies with the x- and y- values. If it is not touched, the z- value will be around 0 as it is connected to the ground. The touch panel is placed on the plate, and the controller is connected on the bottom side of the plate.

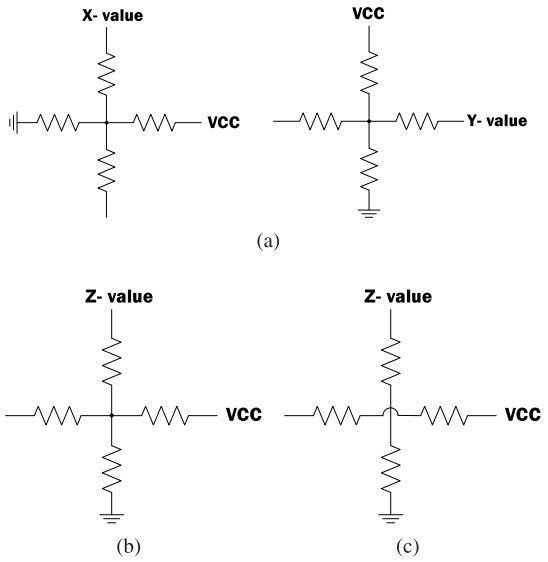

FIGURE 5. Diagram of reading ADC values: (a) x- and y- values, (b) z- value when panel is touched, (c) z- value when panel is not touched.

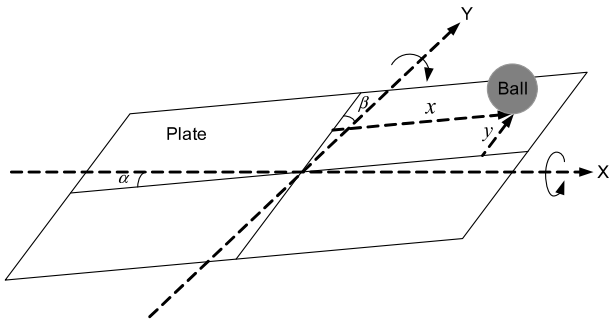

FIGURE 6. Diagram of a ball and plate system.

III. MODEL EQUATIONS AND KINEMATIC ANALYSIS

A. MATHEMATICAL MODEL OF THE BALL AND PLATE SYSTEM

Fig. 6 shows the conceptual diagram for a ball and plate system. The dynamics of a ball and plate system [6] are given by

$$\left(m + \frac{I}{r^2}\right)\ddot{x} - m(x\dot{\alpha}^2 + y\dot{\alpha}\dot{\beta}) + mg\sin\alpha = 0, \quad (1)$$

$$\left(m + \frac{I}{r^2}\right)\ddot{y} - m(y\dot{\beta}^2 + x\dot{\alpha}\dot{\beta}) + mg\sin\beta = 0, \quad (2)$$

where m is the mass of the ball, g is gravity, I is inertia, r is the radius of the ball, and x, y, and α, β are the positions of the ball and the angle of the plate, respectively.

In general, the dynamics of the ball and plate system can be linearized under the following assumptions as in [6], [9], and [16]:

- The rotational angle of the plate is small so that we can assume $\sin\alpha \approx \alpha$ and $\sin\beta \approx \beta$.
- Centrifugal force on the ball may be ignored as it is very small compared to gravity.

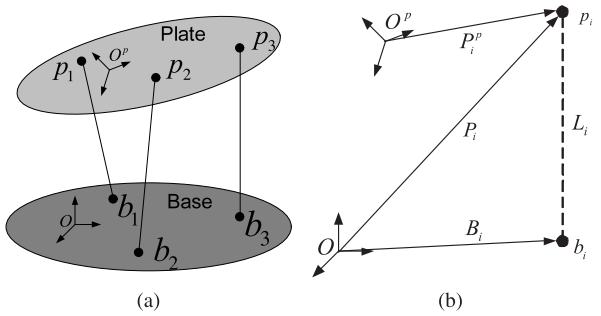

FIGURE 7. Schematic illustration of a Stewart platform. (a) shows the different coordinate system of the plate and the base. (b) shows the relationship of the vectors used in this paper.

From these assumptions, the linearized model can be expressed as follows:

$$\ddot{x} + \frac{5}{7}g\alpha = 0, \tag{3}$$

$$\ddot{y} + \frac{5}{7}g\beta = 0. \tag{4}$$

Equations (3) and (4) are decoupled so that we can consider them as 2 different single input and single output systems. We also can design a controller considering only one system and then apply it to both systems due to their similarity. The input and output for each system are α, x, and β, y.

B. KINEMATICS ANALYSIS OF A STEWART PLATFORM

For the Stewart platform, prismatic actuators are commonly used. However it is either difficult or costly to make a small platform using prismatic actuators. So we use rotary actuators, which means we can make the actuation part using servo motors and horns. The input of the system is the angle of the plate, which is the reason why we need to carry out inverse-kinematics analysis. We use an analysis method similar to that in [17]. The rotation matrix R_b and the translation matrix T_b vary in accordance with the angle and position of the plate. Fig. 7 shows the relationship between the position vector P_i of joints attached to the plate and the length of virtual legs L_i. These variables are calculated as

$$\begin{aligned} P_i &= R_b P_i^p + T_b, \\ L_i &= P_i - B_i = R_b P_i^p + T_b - B_i, \end{aligned} \tag{5}$$

where

$$\begin{aligned} B_i &= \begin{bmatrix} x_i & y_i & z_i \end{bmatrix}^T \\ &= \begin{bmatrix} r_b \cos r_i + r_d \sin r_{ti} & r_b \sin r_i + r_d \cos r_{ti} & 0 \end{bmatrix}^T, \\ P_i^p &= \begin{bmatrix} x_i^p & y_i^p & z_i^p \end{bmatrix}^T = \begin{bmatrix} r_p \cos r_i^p & r_p \sin r_i^p & 0 \end{bmatrix}^T. \end{aligned} \tag{6}$$

Here, B_i is a position vector of the rotation center of each servo motor, r_b is the radius of the circle shown in Fig. 8, r_i is the angle between the x-axis and the line that crosses the origin and the point where the end of the base meet the center line of the servo motor, r_{ti} is the angle of the servo motor,

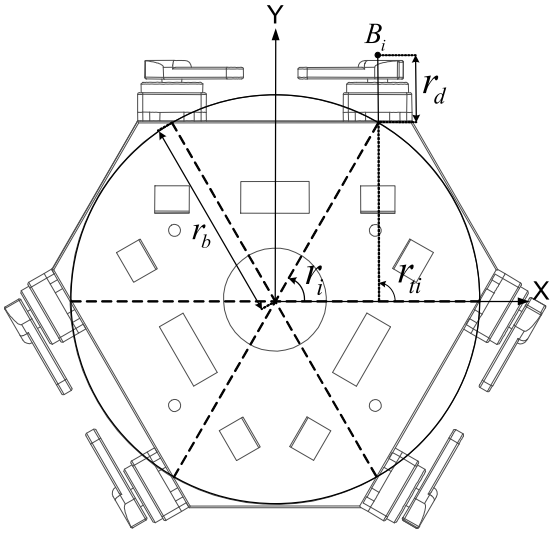

FIGURE 8. Meanings of the vector B_i and the angles.

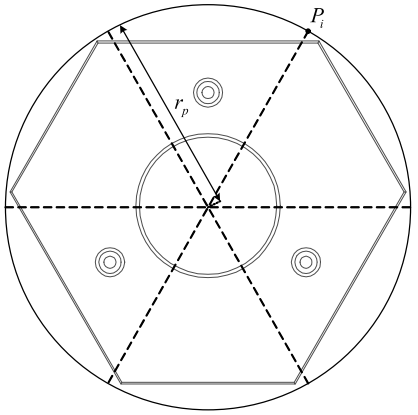

FIGURE 9. Plate and the meaning of the vector P_i.

TABLE 1. Values of the angles.

	1st	2nd	3rd	4th	5th	6th
r_i	60°	120°	180°	240°	300°	360°
r_i^p	45°	135°	165°	255°	285°	15°
r_{ti}	0°	0°	120°	120°	180°	180°

r_d is the distance from the end of the base to the center of a joint attached to the horn, P_i^p is a position vector of a joint attached to the plate in the relative coordinate system of the plate, r_p is the distance from the center of a joint to the origin of the plate shown in Fig. 9, r_i^p is the angle of joints attached to the plate, and subscript i represents the number indicating the servo motor related to each notation. The angles used in this paper are shown in TABLE 1.

L_i is the length made by the prismatic actuators. But, as we use rotary actuators, the rotation angle of the servo motors should be calculated from L_i. Here, we find the position

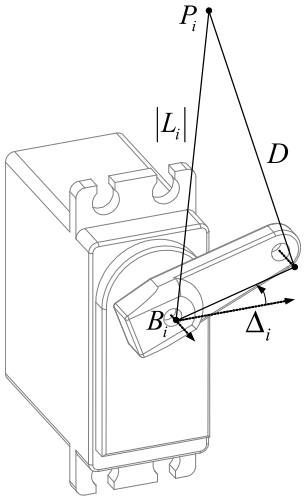

FIGURE 10. Meanings of the variables and constants involved in the computation of the length of a virtual leg L_i.

vector M_i of joints attached to the horns. Then, the equation is given by

$$M_i = \begin{bmatrix} x_{mi} \\ y_{mi} \\ z_{mi} \end{bmatrix} = \begin{bmatrix} x_i \\ y_i \\ z_i \end{bmatrix} + R_z(r_t)R_y(\mp\triangle_i)\begin{bmatrix} \mp R_m \\ 0 \\ 0 \end{bmatrix}, \tag{7}$$

where R_m is the length of the horn. The rotation matrices are given as follows:

$$R_y(\theta) = \begin{bmatrix} \cos\theta & 0 & -\sin\theta \\ 0 & 1 & 0 \\ \sin\theta & 0 & \cos\theta \end{bmatrix},$$
$$R_z(\theta) = \begin{bmatrix} \cos\theta & -\sin\theta & 0 \\ \sin\theta & \cos\theta & 0 \\ 0 & 0 & 1 \end{bmatrix}. \tag{8}$$

$\triangle_i$ is the angle of the i-th servo motor and can be found using the equation at the end of this section. Substituting (8) into (7), M_i can be expressed as follows:

$$M_i = \begin{bmatrix} \pm\cos\triangle_i \cos r_t R_m + x_i \\ \pm\cos\triangle_i \sin r_t R_m + y_i \\ \sin\triangle_i R_m + z_i \end{bmatrix} \equiv M_i(\triangle_i). \tag{9}$$

As shown in Fig. 10, the lengths R_m, D, and $|L_i|$ have relationships with driven vectors as follows:

$$\begin{aligned} R_m^2 &= (M_i(\triangle_i) - B_i)^T(M_i(\triangle_i) - B_i), \\ D^2 &= (P_i - M_i(\triangle_i))^T(P_i - M_i(\triangle_i)), \\ |L_i|^2 &= (P_i - B_i)^T(P_i - B_i), \end{aligned} \tag{10}$$

where D is the length of the leg. By substituting (10) into (9), we can simply express the equation as

$$\pm c_i = a_i \sin\triangle_i + b_i \cos\triangle_i, \tag{11}$$

where

$$\begin{aligned} a_i &= 2R_m(z_i^p - z_i), \\ b_i &= 2R_m((x_i^p - x_i)\cos r_{ti} + (y_i^p - y_i)\sin r_{ti}), \\ c_i &= |L_i|^2 - D^2 + R_m^2. \end{aligned} \tag{12}$$

From (11), we can finally get the angles of each servo motor as follows:

$$\triangle_i = \sin^{-1}\left(\frac{\pm c_i}{\sqrt{a_i^2 + b_i^2}}\right) - \tan^{-1}\left(\frac{b_i}{a_i}\right). \tag{13}$$

Using (12) and (13), $\triangle_i$ is calculated and applied to the i-th servo motor at every sampling time.

IV. DESIGN AND SIMULATION OF THE SMC

A. CONTROLLER DESIGN

The SMC is a nonlinear robust state-feedback control theory that requires a state-space model. Define

$$x_1 = x - x_d, \quad x_2 = \dot{x} - \dot{x}_d,$$

where x_d is the desired position on the $x-$axis. Then, from (3), the state-space model can be described as follows:

$$\begin{bmatrix} \dot{x}_1 \\ \dot{x}_2 \end{bmatrix} = \begin{bmatrix} 0 & 1 \\ 0 & 0 \end{bmatrix}\begin{bmatrix} x_1 \\ x_2 \end{bmatrix} + \begin{bmatrix} 0 \\ -\frac{5}{7}g \end{bmatrix} u. \tag{14}$$

As the system has 2 states, we can design a sliding line as

$$S = \eta x_1 + x_2, \tag{15}$$

where S is the sliding line, and c is the inclination of the line. Using this sliding line, the ball and plate system can be stabilized if the base is horizontal to the ground; unfortunately, most experimental environments are not exactly horizontal to the ground. In order to solve this problem, we design an augmented model of the ball and plate system and use the sliding surface that includes error integration.

$$\begin{bmatrix} \dot{x_1} \\ \dot{x_2} \\ \dot{x_3} \end{bmatrix} = \begin{bmatrix} 0 & 1 & 0 \\ 0 & 0 & 1 \\ 0 & 0 & 0 \end{bmatrix}\begin{bmatrix} x_1 \\ x_2 \\ x_3 \end{bmatrix} + \begin{bmatrix} 0 \\ 0 \\ -\frac{5}{7}g \end{bmatrix} u, \tag{16}$$

where x_1 is the integration of the error, x_2 is the position error, and x_3 is the derivative of the error. We set a sliding surface as follows:

$$S = \eta_1 x_1 + \eta_2 x_2 + x_3, \tag{17}$$
$$\dot{S} = \eta_1 x_2 + \eta_2 x_3 - \frac{5}{7}gu, \tag{18}$$

where η_1 and η_2 are positive coefficients. In general, the control input of the SMC includes the signum function to change variables along the sliding surface. However, high frequency oscillation, which is called chattering, occurs due to the signum function. In this paper, we use a sigmoid-like function to reduce chattering. In order to meet the sliding mode condition, control input is given by

$$u = \frac{7}{5g}\left(\eta_1 x_2 + \eta_2 x_3 + K\sigma(S)\right), \tag{19}$$

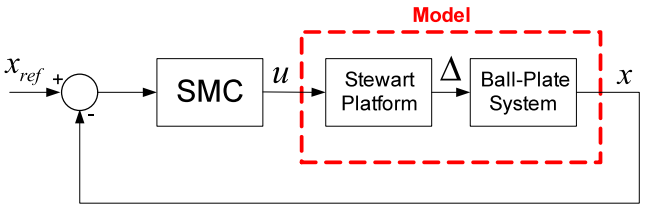

FIGURE 11. SMC scheme of the proposed system.

$$\sigma(S) = \frac{S}{|S| + \delta}, \tag{20}$$

where K is a positive coefficient, δ is a small positive coefficient, and $\sigma(S)$ is a sigmoid-like function. From (17) through (20), we can obtain the following equation, which satisfies the sliding mode condition.

$$S\dot{S} = -KS\sigma(S) = -K\frac{S^2}{|S| + \delta} < 0 \tag{21}$$

Stability of the designed SMC can be verified using Lyapunov stability criteria. As we set the Lyapunov function V as $V = \frac{1}{2}S^2$, we have

$$\dot{V} = S\dot{S}. \tag{22}$$

Here, V is positive definite, and $\dot{V}$ is negative definite from (21). Accordingly, trajectory of the states converges to the sliding surface. To ensure the stability of the system, we need to check whether the trajectory converges to the origin or not when S is zero. By denoting the sliding surface (16) in terms of the error e, it can be expressed as follows:

$$S = \eta_1 \int e + \eta_2 e + \dot{e}. \tag{23}$$

Let $\dot{\psi} = e$. If S is zero, we then obtain the following differential equation:

$$\ddot{\psi} + \eta_2\dot{\psi} + \eta_1\psi = 0. \tag{24}$$

The characteristic equation of (24) can be described as follows:

$$\lambda^2 + \eta_2\lambda + \eta_1 = 0, \tag{25}$$

where λ is a solution of the characteristic equation. As η_2 is positive, we can get

$$Re(\lambda) = -\frac{\eta_2}{2} < 0. \tag{26}$$

Therefore, the control system is asymptotically stable.

B. SIMULATION

The SMC scheme is shown in Fig. 11. First, we conducted simulation to compare the SMC using a basic sliding line with the SMC that includes integration of error. We assumed that there exists external disturbance to the control input as the base of the system may not be horizontal to the ground in real situations. We applied disturbance of 0.05 radian to α and that of -0.07 radian to β. As a result, as shown in

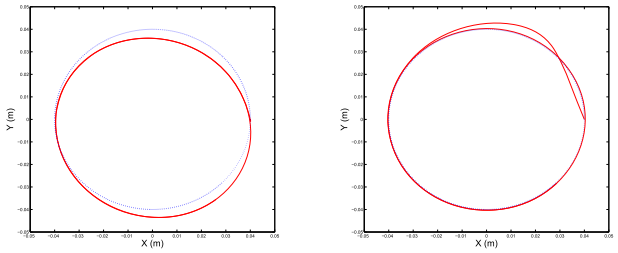

(a) (b)

FIGURE 12. Comparison of two different SMCs. (a) The one using a normal sliding line. (b)The one with integration error.

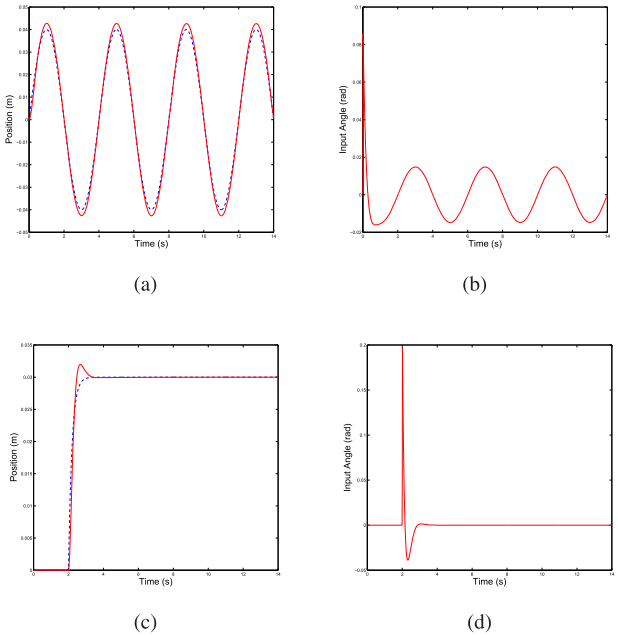

(a) (b) (c) (d)

FIGURE 13. Performance of the designed SMC. (a) Tracking smooth reference: the position of the ball(solid) and the reference(dash). (b) Control input of (a). (c) Tracking step reference: the position of the ball(solid) and the reference(solid). (d) Control input of (c).

(a) of Fig. 12, the ball immediately showed a steady-state response, but it did not draw a concentric circle with the reference circle. On the other hand, the ball exactly followed its desired path, as shown in (b), though there was some transient response at the beginning. The red line in Fig. 12 is the trajectory of the ball, and the blue dotted line is the reference trajectory. To illustrate the performance of the designed SMC, we conducted simulation using the augmented model in (16) for tracking the sine reference and step reference. We set $\eta_1 = 3.85$, $\eta_2 = 4.4$, $K = 1.95$, and $\delta = 4.5$.

Results of the simulation are shown in Fig. 13. There, (a) is the the result of tracking a sine reference whose period is 4 seconds. The maximum errors in (a) and (c) are about 3mm each. These maximum errors occur when the ball changes direction as the system cannot react fast without a predicted trajectory. The graphs of the input in (b) and (d) of Fig. 13 show that there is no chatter.

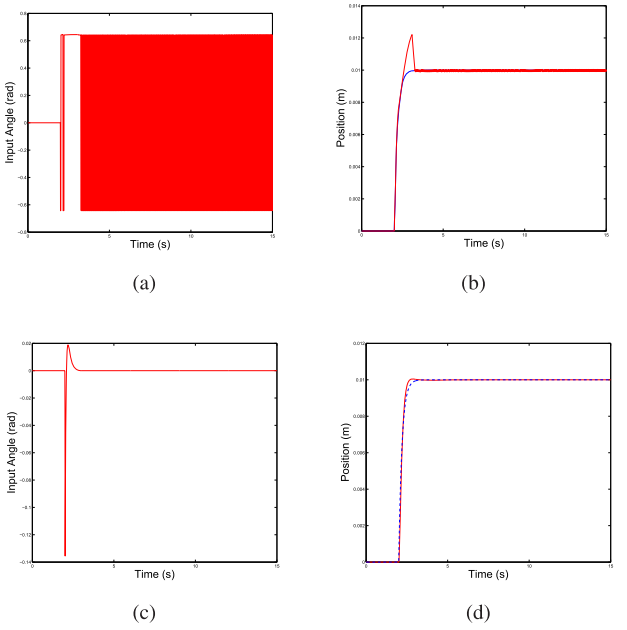

FIGURE 14. Comparison of two SMCs that use different functions to the control input. (a) Control input using a signum function. (b) System output of (a). (c) Control input using a sigmoid-like function. (d) System output of (c).

In addition, we conducted simulation to see the effect of the sigmoid-like function in the control logic. (a) in Fig. 14 is a control input using the signum function and (c) is the one using the sigmoid-like function. (b) and (d) are the position of the ball in case of (a) and (c), respectively. Simulations were conducted under the same condition. As shown in (a), there exists chattering because the signum function changes the value discontinuously near the origin. On the other hand, as shown in (c), if we use sigmoid-like function, chattering is barely shown. Those two cases seem working, because both (b) and (d) show that the ball tracks the reference well. However, it is impossible to apply the control input as in (a) of Fig. 14, since the control input of the system is the angle of the plate. Physically, the angle cannot be changed in high frequency as shown in (a). Therefore, using sigmoid-like function is reasonable for the proposed system.

V. EXPERIMENT

We used the same coefficients as in the simulation. First, we performed the control experiments using LQ control and SMC. The results of these tracking performances are shown in Fig. 15. The radius of the circular trajectory is 4cm and the ball draws one circle in 8 seconds in (b) and (e), and in 4 seconds in (d) and (h). Vibration in the trajectory is more likely when the velocity is small. The maximum errors of (e) and (g) are 2mm and 4mm, respectively. On the other hand, the maximum errors of (a) and (c) are 5mm and 12 mm, respectively.These tendencies also occurred in the simulation. From this experiment, we found that SMC normally works better than LQ control for a ball and plate system because the maximum error of the LQ control tends to become larger than that of SMC as the velocity is increased.

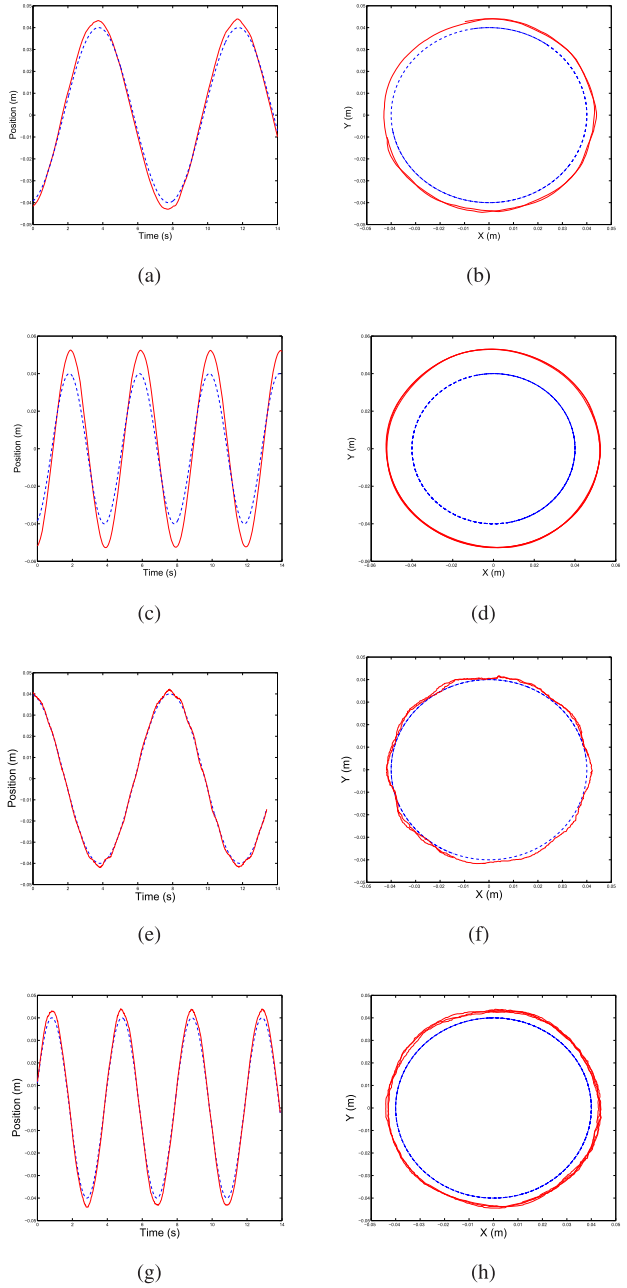

FIGURE 15. Comparison of the tracking performance. (a) Position X of LQ control with a period of 8 seconds. (b) X-Y plane of LQ control with a period of 8 seconds. (c) Position X of LQ control with a period of 4 seconds. (d) X-Y plane of LQ control with a period of 4 seconds. (e) Position X of SMC with a period of 8 seconds. (f) X-Y plane of SMC with a period of 8 seconds. (g) Position X of SMC with a period of 4 seconds. (h) X-Y plane of SMC with a period of 4 seconds.

VI. CONCLUSIONS

In this paper, we proposed an implementation method of a ball and plate control system as an education kit. The proposed system includes a Stewart platform with 6 servo motors as an actuation part and a 10.2 in. touch panel as a sensor. The

main controller for the system is the Nucleo-32 board, which is small and powerful open-source hardware. Using these parts, the system can be made at low cost and does not need any extra instruments, which means it is efficient to provide a control system for students in a lecture. The mathematical model of the ball and plate system was given, and the kinematics analysis of the Stewart platform was explained in detail. We conducted simulations and experiments using SMC. We showed the performance of the SMC and compared it with that of the LQ control. From the experiment, we demonstrate that the system is well-made with the proposed method and can be applied to study various controllers.

REFERENCES

[1] C. J. Bay and B. P. Rasmussen, "Exploring controls education: A re-configurable ball and plate platform kit," in *Proc. Amer. Control Conf. (ACC)*, Boston, MA, USA, Jul. 2016, pp. 6652–6657.
[2] R. M. Reck and R. S. Sreenivas, "Developing a new affordable DC motor laboratory kit for an existing undergraduate controls course," in *Proc. Amer. Control Conf. (ACC)*, Chicago, IL, USA, Jul. 2015, pp. 2801–2806.
[3] D. Schinstock, S. Schinstock, and W. N. White, "Micro-controller based update of inexpensive undergraduate control systems laboratory hardware," in *Proc. Amer. Control Conf. (ACC)*, Chicago, IL, USA, Jul. 2015, pp. 2807–2812.
[4] T. Meta, G. Y. Gyeong, J. H. Park, and Y. S. Lee, "Swing-up control of an inverted pendulum subject to input/output constraints," *J. Inst. Control, Robot. Syst.*, vol. 20, no. 8, pp. 835–841, 2014.
[5] J. S. Choi and Y. S. Lee, "The implementation of a hardware-in-the-loop simulator for an inverted pendulum system using open-source hardware," *J. Inst. Control, Robot. Syst.*, vol. 23, no. 2, pp. 117–125, 2017.
[6] L. Spacek and V. Bovál, and J. Vojtesek, "Digital control of Ball and Plate model using LQ controller," in *Proc. 21st Int. Conf. Process Control (PC)*, Strbske Pleso, Slovakia, Jun. 2017, pp. 36–41.
[7] H. Liu and Y. Liang, "Trajectory tracking sliding mode control of ball and plate system," in *Proc. 2nd Int. Asia Conf. Inform. Control, Autom. Robot. (CAR)*, Wuhan, China, vol. 3, Apr. 2010, pp. 142–145.
[8] X. Fan, N. Zhang, and S. Teng, "Trajectory planning and tracking of ball and plate system using hierarchical fuzzy control scheme," *Fuzzy Sets Syst.*, vol. 144, no. 2, pp. 297–312, 2004.
[9] Z. Fei, Q. Xiaolong, L. Xiaoli, and W. Shangjun, "Modeling and PID neural network research for the ball and plate system," in *Proc. Int. Conf. Electron., Commun. Control (ICECC)*, Ningbo, China, Sep. 2011, pp. 331–334.
[10] C. I. Huang, C.-F. Chang, M.-Y. Yu, and L.-C. Fu, "Sliding-mode tracking control of the Stewart platform," in *Proc. 5th Asian Control Conf.*, vol. 1, Melbourne, VIC, Australia, 2004, pp. 562–569.
[11] G. Bartolini, A. Pisano, E. Punta, and E. Usai, "A survey of applications of second-order sliding mode control to mechanical systems," *Int. J. Control*, vol. 76, nos. 9–10, pp. 875–892, Jan. 2003.
[12] H.-T. Yau and C.-L. Chen, "Chattering-free fuzzy sliding-mode control strategy for uncertain chaotic systems," *Chaos, Solitons Fractals*, vol. 30, no. 3, pp. 709–718, Nov. 2006.
[13] J. Baek, M. Jin, and S. Han, "A new adaptive sliding-mode control for rigid robotic manipulators," *IEEE Trans. Ind. Electron.*, vol. 63, no. 6, pp. 3628–3637, Jun. 2016.
[14] H. Li, J. Wang, H. Du, and H. R. Karimi, "Adaptive sliding mode control for Takagi–Sugeno fuzzy systems and its applications," *IEEE Trans. Fuzzy Syst.*, vol. 26, no. 2, pp. 531–542, Apr. 2018.
[15] D. S. Bernstein, "Enhancing undergraduate control education," *IEEE Control Syst.*, vol. 19, no. 5, pp. 40–43, Oct. 1999.
[16] A. Knuplez, A. Chowdhury, and R. Svecko, "Modeling and control design for the ball and plate system," in *Proc. IEEE Int. Conf. Ind. Technol.*, Maribor, Slovenia, Dec. 2003, pp. 1064–1067.
[17] F. Szufnarowski, "Stewart platform with fixed rotary actuators: A low cost design study," in *Advances in Medical Robotics*, 1st ed. Univ. Rzeszów, Rzeszów, Poland, 2013, ch. 4.

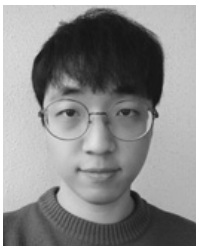

HEESEUNG BANG received the B.S. degree in mechanical engineering from Inha University, Incheon, South Korea, in 2018. He is currently pursuing the M.S. degree in electrical engineering with Inha University, Incheon, South Korea. His research interests include nonlinear control, parallel robot, and embedded systems.

YOUNG SAM LEE received the B.S. and M.S. degrees in electrical engineering from Inha University, Incheon, South Korea, in 1999, and the Ph.D. degree in electrical engineering from Seoul National University, South Korea, in 2003. From 2003 to 2004, he was a Senior Researcher with Samsung Electronics Company. Since 2004, he has been with the Department of Electrical Engineering, Inha University, Incheon, South Korea. He has authored four books and over 50 articles. His research interests include computer-aided control system designs, rapid control prototyping, control and instrumentation, robot engineering, and embedded systems.